Applied Microbiology and Biotechnology (2024) 108:444
https://doi.org/10.1007/s00253-024-13240-0

BIOTECHNOLOGICALLY RELEVANT ENZYMES AND PROTEINS

Transcriptional and secretome analysis of *Rasamsonia emersonii* lytic polysaccharide mono-oxygenases

Yashika Raheja[1] · Varinder Singh[1] · Nitish Kumar[2] · Dhruv Agrawal[1] · Gaurav Sharma[1] · Marcos Di Falco[3] · Adrian Tsang[3] · Bhupinder Singh Chadha[1]

Received: 2 October 2023 / Revised: 10 June 2024 / Accepted: 14 June 2024 / Published online: 21 August 2024

Abstract

The current study is the first to describe the temporal and differential transcriptional expression of two lytic polysaccharide monooxygenase (LPMO) genes of *Rasamsonia emersonii* in response to various carbon sources. The mass spectrometry based secretome analysis of carbohydrate active enzymes (CAZymes) expression in response to different carbon sources showed varying levels of LPMOs (AA9), AA3, AA7, catalase, and superoxide dismutase enzymes pointing toward the redox-interplay between the LPMOs and auxiliary enzymes. Moreover, it was observed that cello-oligosaccharides have a negative impact on the expression of LPMOs, which has not been highlighted in previous reports. The LPMO1 (30 kDa) and LPMO2 (47 kDa), cloned and expressed in *Pichia pastoris*, were catalytically active with (k_{cat}/K_m) of 6.6×10^{-2} mg^{-1} ml min^{-1} and 1.8×10^{-2} mg^{-1} ml min^{-1} against Avicel, respectively. The mass spectrometry of hydrolysis products of Avicel/carboxy methyl cellulose (CMC) showed presence of C_1/C_4 oxidized oligosaccharides indicating them to be Type 3 LPMOs. The 3D structural analysis of LPMO1 and LPMO2 revealed distinct arrangements of conserved catalytic residues at their active site. The developed enzyme cocktails consisting of cellulase from *R. emersonii* mutant M36 supplemented with recombinant LPMO1/LPMO2 resulted in significantly enhanced saccharification of steam/acid pretreated unwashed rice straw slurry from PRAJ industries (Pune, India). The current work indicates that LPMO1 and LPMO2 are catalytically efficient and have a high degree of thermostability, emphasizing their usefulness in improving benchmark enzyme cocktail performance.

Key points

- *Mass spectrometry depicts subtle interactions between LPMOs and auxiliary enzymes.*
- *Cello-oligosaccharides strongly downregulated the LPMO1 expression.*
- *Developed LPMO cocktails showed superior hydrolysis in comparison to CellicCTec3.*

Keywords *Rasamsonia emersonii* · LPMOs · In silico modeling · Mass spectrometry · Hydrolysis

✉ Bhupinder Singh Chadha
chadhabs@yahoo.com

Yashika Raheja
yashikamicro.rsh@gndu.ac.in

Varinder Singh
varinder75@gmail.com

Nitish Kumar
nitishpharma.rsh@gndu.ac.in

Dhruv Agrawal
dhruvagrawal782@gmail.com

Gaurav Sharma
gauravmicro.rsh@gndu.ac.in

Marcos Di Falco
marcos.difalco@concordia.ca

Adrian Tsang
adrian.tsang@concordia.ca

[1] Department of Microbiology, Guru Nanak Dev University, Amritsar-143005, Punjab, India

[2] Department of Pharmaceutical Sciences, Guru Nanak Dev University, Amritsar, India

[3] Center for Structural and Functional Genomics, Concordia University, 7141 Sherbrooke Street West, Montreal, Quebec H4B 1R6, Canada

Introduction

Lignocellulosic biomass (LCB) is a copious carbon neutral resource comprising of cellulose and hemicellulose fibers that are convolved and embedded in a dense polymer matrix of lignin, conferring it a recalcitrant attribute (Zhang et al. 2021a). Due to structural intricacy of LCB, it requires pretreatment to bring about disintegration and fractionation of its complex structure into cellulose, hemicellulose, and lignin for its efficient valorisation. The pretreated LCB is subsequently subjected to hydrolysis where a spectrum of lignocellulolytic enzymes synergistically act on the cellulose fibers to convert them into monomeric glucose moieties (Vaaje-Kolstad et al. 2010; Sharma et al. 2022). The extent of hydrolysis that can be achieved depends on structural complexity of the substrate as well as the catalytic efficacy of enzymes. However, the catalytic efficiency of enzymes is compromised due to the presence of inhibitors (hydroxy methyl furfurals (HMF), acetic acid, formic acid, levulinic, ferulic acid, etc.) in the acid/steam pretreated unwashed slurry, negatively impacting enzyme action and resulting in lower glucan hydrolysis (~ 60%) at enzyme loading rates of 10 mg/g substrate and solid concentrations of 15–17% (Dessie et al. 2019; Cavalaglio et al. 2021; Hoppert et al. 2022). Therefore, in order to achieve desired hydrolysis levels (>90%), higher amounts of enzyme (30 mg/g substrate) are required, making the process commercially uneconomical (Reis et al. 2023).

The deconstruction of lignocellulosic biomass, which was solely attributed to the hydrolytic action of glycosyl hydrolases previously, has seen a paradigm shift with discovery of oxidative lytic polysaccharide monooxygenases (LPMOs) (Horn et al. 2012). These LPMOs display a redox-potential-mediated catalysis to initiate the rapid disintegration of the crystalline lattice surface of cellulose, which is otherwise not easily accessible to canonical glycosyl hydrolases (Chylenski et al. 2019). The catalytic cycle of LPMO action is initiated by the reduction of Cu(II) from its resting state to Cu(I) in the presence of co-substrate (H_2O_2) which results in the generation of super-oxo species. The released super-oxo species then is converted to copper(II)-hydro-per-oxo, followed by the homolytic cleavage of the O-O bond. This oxygen-oxygen bond breakage releases Cu−oxyl reactive species and oxidizes the polysaccharide at different positions based on their regioselectivity (either C_1, C_4, or both). The LPMOs are categorized in three different classes, where Type 1 LPMOs carry out oxidative cleavage at C_1 of glycosidic unit, Type 2 LPMOs oxidatively cleave at C_4 and Type 3 LPMOs oxidatively cleave both at the C_1 and C_4 positions (Bertini et al. 2018; Ma et al. 2021). Although the first reduction reaction involved in LPMO-mediated catalysis is substrate dependent, however, LPMOs acting on lignin rich biomass do not require the external addition of electron donors. The presence of low molecular weight lignin compounds itself act as electron carrier between the polymer and the enzyme (Kont et al. 2019) to carry out the oxidative cleavage. The secretome of several biomass degrading fungi had previously revealed the presence of auxiliary enzymes cellobiose dehydrogenase (CDH; AA8), AA3, AA7 (oligosaccharide oxidase) that are involved in direct electron transfer and supports the potential interplay between these enzymes (Manavalan et al. 2021). However, the external source of electron donors under the lab conditions mostly consists of ascorbic acid, gallic acid and methyl hydroquinone that supports H_2O_2 driven oxidation of biomass by LPMOs (Garajova et al. 2016; Momeni et al. 2021). The addition of H_2O_2 exogenously or its in situ generation during pretreatment of lignocellulosics has been reported to aid in LPMO-mediated catalysis (Müller et al. 2018).

Despite the recent progress in structural analysis, substrate specificity, and regioselectivity of LPMOs; not much is known about functional determinants which governs the induction of LPMO expression in the presence of complex polysaccharides. Indeed, the incorporation of LPMOs in a cellulase mixture increases hydrolysis, but its activation requires artificial/enzyme donors such as ascorbate, gallic acid, auxiliary enzymes such as CDH (AA8), AA3_2, AA7, and other class of oxidoreductases, which pose a major challenge for its endorsement by future biorefineries (Garajova et al. 2016; Johansen 2016; Østby et al. 2020). Yet, the insight into the redox interplay between the LPMOs and other class of oxidative enzymes remains shrouded. Genome wide sequence analysis in recent times has shown that LPMO coding genes are very well represented components of CAZymes, and their synergism with other glycosyl hydrolases forms an important step in designing optimal cellulase enzyme mixture with better performance in comparison to the present commercial lignocellulolytic blends. The genome wide databases suggest that the organisms host a diverse number of LPMO genes. However, the paucity of knowledge about how many and to what extent these LPMOs are induced and expressed under the process parameters employed during fermentation by the producer strains is an intriguing aspect. As all the LPMOs are not expressed during production of CAZymes, therefore, bioprospecting the catalytic potential of LPMOs that remain silenced during culturing can be addressed using heterologous gene expression platforms, followed by their purification and characterization so as to identify potentially useful LPMOs for the formulation of potent custom-designed enzyme cocktails.

In the present work, cloning, expression, and characterization of two LPMO (AA9) genes from *Rasamsonia emersonii* using *Pichia pastoris* as a host was carried out to identify and compare their catalytic efficacy. The present study also provides the first report on transcriptional profiling of both the LPMO genes that are present in the genome of *R. emersonii* and aims at portraying the interplay between the LPMOs (AA9) and other auxiliary enzymes with specific emphasis on fine-tuned induction in presence of different polysaccharides. Furthermore, the hydrolytic performance of in-house custom-made cocktails consisting of *R. emersonii* secretome and heterologously expressed recombinant LPMOs was evaluated for the hydrolysis of biorefinery relevant inhibitors laden unwashed steam/acid pretreated rice straw slurry procured from 2G ethanol demonstration plant (PRAJ, Pune, India) and compared with the commercial enzyme CellicCtec3 (Novozymes, Bagsværd, Denmark).

Materials and methodology

Microbial strains and growth media

The thermophilic fungus *R. emersonii* (collection number MTCC-387) was employed as a source of LPMO in this study (Raheja et al. 2022). *R. emersonii* was regularly maintained and grown on *Talaromyces* agar medium comprising of cellulose 3%, wheat grain flour 1.5%, bactopeptone 0.75%, potassium dihydrogen phosphate (KH_2PO_4) 0.5%, calcium chloride dihydrate ($CaCl_2.2H_20$) 0.05%, and salt fraction 1.5% at 44°C (Raheja et al. 2020). Bacterial culture of *Escherichia coli* (Top10F strain, Invitrogen, Waltham, MA, USA) and *P. pastoris* (X-33 strain, Invitrogen, Waltham, MA, USA) was used for cloning and overexpression. Low-salt LB media (tryptone 1%, yeast extract 0.5%, and NaCl 0.5%) supplemented with antibiotic zeocin (25 µg mL^{-1}) was used for the selection of *E. coli* transformants. Yeast strain *P. pastoris* was maintained on YPD medium (yeast extract 1%, peptone 2%, and dextrose 2%).

Cloning and overexpression of LPMO1 and LPMO2 genes in *P. pastoris*

The gene sequences for both the LPMOs Talem1p7_017256 (*LPMO1*) and Talem1p7_002983 (*LPMO2*) were downloaded from a fungal genome portal (https://genome.jgi.doe.gov/portal/). The lignocellulolytic enzyme induction was carried out by growing *R. emersonii* on an optimized medium (Raheja et al. 2020). The total RNA was extracted using a HiPurA™ RNA purification kit (Himedia, Mumbai, India) followed by mRNA enrichment (mRNA isolation kit, Invitrogen, Waltham, MA, USA) and cDNA synthesis (Agrawal et al. 2020b). Based on the gene sequences, open reading frame (ORF) specific primers with *Eco*RI and *Xba*I restriction sites were designed for *LPMO1* and *LPMO2* (Supplemental Table S1). The amplification of the desired genes using cDNA as a template was carried out using high fidelity Q5® DNA Polymerase (New England Biolabs, Ipswich, MA, USA) with initial denaturation at 98°C for 40 s, 35 cycles of denaturation at 98°C for 15 s, annealing at 54°C for 45 s, extension at 72°C for 1 min 30 s followed by final extension at 72°C for 5 min. The size for resultant amplified products was verified by agarose gel electrophoresis (1% w/v) followed by purification using Gel Extraction Kit (Sigma, St. Louis, MO, USA). The purified amplicons were digested with *Eco*RI and *Xba*I enzymes followed by ligation into *Eco*RI and *Xba*I digested pPICZαA (Invitrogen, Waltham, MA, USA) plasmid (Hong et al. 2007). The plasmids containing AA9 genes were then transformed into chemically competent cells of Top10F *E. coli* (Invitrogen, Waltham, MA, USA) by heat shock at 42°C for 1 min followed by plating on low-salt LB agar plates containing selectable marker zeocin. Transformants were screened for cloning using colony PCR and double digestion by *Eco*RI and *Xba*I restriction enzymes. Positive transformants were further used for isolating the plasmid followed by linearization using *Pme*I (New England Biolabs, Ipswich, MA, USA). The linearized plasmids were then transformed via electroporation (Invitrogen, Carlsbad, CA, USA) into freshly prepared competent cells of *P. pastoris* X-33 and subsequently plated onto YPDS medium (1% yeast extract; 2% peptone; 2% dextrose and 1 M sorbitol) containing 100 µg/mL zeocin (Mellitzer et al. 2012). The obtained transformants were screened for expression of the desired gene using the protocol mentioned in the EasySelect™ *Pichia* Expression Kit manual (Invitrogen, Waltham, MA, USA) that involved feeding of the culture flasks with 1% (v/v) methanol, for the induction of AOX promoter, at 24 h intervals with the first feed starting after 48 h upto 120 h (Basotra et al. 2019). The resultant culture supernatants were subjected to centrifugation (3000 ×g, 5 min) and subsequently assayed for LPMO activity using 2% (w/v) carboxymethyl cellulose (CMC) as substrate (Karlsson et al. 2001; Agrawal et al. 2020b). The reaction mixture containing 500 µL of diluted enzyme was incubated with the 500 µL of substrate (2% CMC) prepared in sodium citrate buffer (50 mM; pH 6.0) for 20 min thereafter the reaction was terminated by the addition of 3 mL 3,5 dinitrosalicylic acid (DNS) followed by boiling at 100°C for 10 min (Miller 1959). The resultant developed color was quantified by measuring the absorbance at 540 nm (Novaspec II, Pharmacia, Delhi, India). Furthermore, the gene cloning was validated by sequencing of PCR amplified products (BioServe, Hyderabad, India). The recombinant strains of LPMO1 (accession

number MTCC13352) and LPMO2 (accession number MTCC13353) used in the present study have been deposited at the Microbial Type Culture Collection and Gene Bank, Chandigarh (India).

Bioinformatics studies and structural analysis of LPMO1 and LPMO2

The protein sequence in FASTA format was obtained from a fungal protein database (https://genome.jgi.doe.gov/portal/) and used for generating 3D structure of the protein by SWISS MODEL (Swiss Institute of Bioinformatics, Basel, Switzerland; Waterhouse et al. 2018). On the basis of the GMQE score (global model quality estimate score) and QMEAN (Quality Model Energy Analysis), the most appropriate model was selected (Pramanik et al. 2021). Homology modeling and multiple sequence alignment for LPMOs was carried out using Schrodinger suite (2018-4, New York, USA; Jacobson et al. 2004) and the crystal structures of *Thermoascus aurantiacus* (2YET) and *Neurospora crassa* (4EIR) were used as templates for LPMO1 and the LPMO2, respectively. The structural superimposition was carried out and Root Mean Square Deviation (RMSD) between the template and models were computed on the basis of homology model scores. Based on the sequence alignment, a phylogenetic tree (neighbor joining) was constructed using Mega X (https://www.megasoftware.net/) (Hoda et al. 2021). Furthermore, molecular docking was performed by protein preparation wizard by capping the termini, assignment of the hydrogen bonds, bond orders, addition of hydrogens, and protein optimization, minimization using the protein prep wizard. Ligand (Avicel) preparation was carried out using LigPrep (Schrodinger 2018-4, New York, USA) and the stereoisomers of each ligand were generated. The ligands with low energy 3D conformations were selected. Using the sitemap tool, the most prominent active sites for substrate binding were predicted in the LPMO protein. The receptor grid was generated (20 × 20 × 20 Å) using the glide grid generation tool and all the ligands were docked using docking module in the glide (grid based ligand docking with energetics) (Dadheech et al. 2019). The best pose of a docked ligand was visualized by the extra-precision module (XP-visualizer) and was selected on the basis of G score and molecular mechanics generalized born surface area (MMGBSA) generated binding energies (Basotra et al. 2019).

Purification of LPMOs and estimation of LPMO activity

Purification of both the LPMOs was performed using an anion exchange chromatographic column UNOsphere™ Q (Bio-Rad, Haryana, India). Before loading the samples onto the column, the crude enzymes (500 mL) from both the LPMOs were concentrated and desalted using an ultrafiltration system (AMICON, Miami, FL, USA) fitted with a 10 kDa cutoff PES membrane (Permionics India Ltd., Gujarat, India). The concentrated enzymes LPMO1 and LPMO2 were in 50 mM Tris buffer (pH 8.0). Five mL of the concentrated protein samples (LPMO1, 52.30 mg/mL; LPMO2, 44.65 mg/mL) were loaded onto a column followed by fractionation through AKTA prime fast protein liquid chromatography (FPLC; GE Healthcare, Chicago, IL, USA). The bound LPMOs were eluted with 50 mM Tris buffer (pH 8.0) using gradient of NaCl (0–100%) with flow rate of 1.0 mL/min. Thereafter, the eluted fractions were assayed for enzymatic activity and further confirmed for purity by 12% SDS-PAGE (Mini-Protein II system, BioRad, Hercules, CA, USA), and the reference molecular marker dual Precision Plus Protein™ (BioRad, Hercules, CA, USA) was used as standard to determine the molecular weight of purified LPMOs. The eluted fractions were profiled by estimating the enzyme activity using CMC as substrate in presence of reductant (1 mM ascorbic acid) (Agrawal et al. 2020a). The protein content in the purified fractions was determined by Lowry's method (Lowry et al. 1951). Furthermore, the LPMO activity in the purified fractions was also determined using a reaction mixture consisting of 860 µL of 116 mM sodium phosphate buffer (pH 7.0), 100 µL of 10 mM 2,6-dimethoxyphenol (2,6-DMP) and 20 µL of 5 mM H_2O_2, which was gently mixed and incubated at 30°C for 15 min. Afterwards, 20 µL of purified enzyme fraction with LPMO1 (0.88 U/mg) and LPMO2 (0.47 U/mg) was added, and the increase in absorption was measured at 469 nm for 5 min using a spectrophotometer (Novaspec II, Pharmacia, Delhi, India) (Breslmayr et al. 2018). All the reactions were performed in triplicates.

Characterization of purified LPMO1 and LPMO2 proteins

The purified proteins were characterized using different parameters including pH, temperature, metal ions, and substrates. Effect of pH on purified enzymes LPMO1 and LPMO2 was studied using a broad range of buffer systems (pH 3.0–12.0), including 50 mM sodium acetate (pH 3.0–5.0), sodium citrate (pH 6.0), sodium phosphate (pH 7.0), Tris chloride (pH 8.0–9.0), and glycine NaOH (pH 10.0–12.0). Enzyme activity was carried out using 2% CMC with 1 mM ascorbic acid as a reducing agent. Similarly, the temperature profiling was studied for both the LPMOs between 20 and 80°C (Agrawal et al. 2020b). Enzyme thermostability was checked using two different parameters, for LPMO1, pH 7.0 and 9.0 and temperatures 50°C and 60°C up to 96 h and for LPMO2, pH 7.0 and 8.0; temperatures 50°C

and 60°C up to 168 h. Furthermore, the different metal ions effects were also evaluated by incubating both the purified LPMOs with different metal ions (5 mM) for 30 min at room temperature and the residual enzymatic activity was assayed using 2% w/v CMC as a substrate in the presence of 1mM ascorbic acid. The substrate specificities of both purified LPMO proteins were studied using a broad range of substrates: Avicel, phosphoric acid swollen cellulose (PASC), CMC, β glucan (barley), starch, laminarin, lichenan, birchwood xylan, beechwood xylan, wheat arabinoxylan, oat spelt xylan, xyloglucan, debranched arabinan, larchwood xylan, and rye arabinoxylan. The concentration of each substrate used was 2% (w/v) prepared in 50 mM Tris chloride buffer with pH 9.0 for LPMO1 and pH 8.0 for LPMO2 applied at 60°C for 2 h. Furthermore, the role of H_2O_2 as a co-substrate for LPMOs was evaluated using a previously published protocol (Bissaro et al. 2017) adopted with some modifications. Estimation was done using Avicel (2% w/v) with addition of different H_2O_2 concentrations (10–100 µM) and 1 mM ascorbic acid prepared in 50 mM Tris chloride buffer pH 9.0 for LPMO1 and pH 8.0 for LPMO2. The reactions were incubated for 2 h at 60°C after which the reactions were filtered (0.45 µm) followed by determination of released reducing sugars using 3,5-dinitrosalicylic acid (DNS) (Agrawal et al. 2020a). The enzyme kinetics (kinetic parameters: K_m, V_{max}, k_{cat}, and k_{cat}/K_m) was studied against Avicel in the presence of 1 mM ascorbic acid as reducing agent and 20 µM of H_2O_2 co-substrate and assayed under standard conditions. All the reactions were performed in triplicates.

Transcriptional profiling and proteomic analysis of LPMO1 and LPMO2

For temporal expression profiling of LPMOs, *R. emersonii* was grown in 250 mL Erlenmeyer flasks containing 50 mL of optimized medium (Raheja et al. 2020) consisting of 4% cellulose, 2% gram flour, 0.75% bactopeptone, 1% KH_2PO_4, 0.05% $CaCl_2.2H_2O$, 1.5% salt fraction, and 0.1% Tween 80 was incubated at 44°C under shaking conditions (250 rpm). Salt fraction used in the study consisted of 0.2% ammonium sulfate, 0.18% potassium chloride (KCl), 0.045% citric acid, 0.1% $CaCl_2.2H_20$, and 0.01% trace element solution {copper sulfate ($CuSO_4$), zinc sulfate ($ZnSO_4$), manganese sulfate ($MnSO_4$), ferrous sulfate ($FeSO_4$)}. Total RNA was isolated from the mycelium of actively growing culture harvested at different time intervals (days) 1, 3, 5, 7, and 9 using Fungal RNA isolation kit (Himedia, Mumbai, India). The isolated RNA was subjected to DNase treatment (Sigma-Aldrich, St. Louis, MO, USA) and cDNA synthesis was carried out using an iScript cDNA synthesis kit (Bio-Rad, St. Louis, MO, USA). The sequences for both the LPMO genes Talem1p7_017256 (*LPMO1*) and Talem1p7_002983 (*LPMO2*) were used for designing qRT-PCR primers (Supplemental Table S1). The detailed protocol used for real-time PCR have been reported previously (Raheja et al. 2022). The elongation factor gene (EF-1, Talem1p7_017962) was used as the reference gene. Furthermore, the differential expression of LPMOs was also studied in media types that contained different carbon sources: A (cellulose; cell) containing 4% cellulose, B (cellulose+glucose; cell+glu); 4% cellulose and 1.5 % glucose, C (acid pretreated rice straw slurry; AcRsPRAJ); 4% acid pretreated rice straw slurry (pH 5.0) procured from PRAJ Industries Ltd, D (endoglucanase hydrolysed acid pretreated rice straw slurry; oligoEG); 4% liquefied rice straw slurry that had been hydrolysed using 200 U/g of mono-component *R. emersonii* endoglucanase (GH5) cloned and expressed in *P. pastoris*, E (untreated rice straw; UnRs) 4% untreated rice straw biomass and F (Avicel; Avi) 4% Avicel (PH-101). The culture extracts obtained after 5 days on different media types were prepared for the exoproteome analysis by protein precipitation with chilled acetone (80%; two volumes). The pellet was suspended in ammonium bicarbonate (0.2 M) with added anionic acid labile surfactant II (0.1% w/v). The obtained protein samples were then resolved on a 12% SDS-PAGE gel and were sliced into pieces. Followed by slicing, in-gel digestion was carried out with trypsin (6 ng/µl). The resultant peptides were extracted by incubating gel pieces multiple times in a 1% formic acid (FA) solution and increasing concentrations of acetonitrile (ACN). In a speedvac, the extracted peptides were dried followed by resuspension in a 5% ACN: 0.1% FA mixture (100 µl). Five microliters of the obtained peptide extract was injected onto a C18 resin (Phenomenex, Torrance, CA) column (12 cm × 75 µm) connected in-line to an LTQ-Velos Orbitrap mass spectrometer (Thermo-Fisher, San Jose, CA). The peptide mixture was separated by generating a linear gradient with a flow rate of 300 nL/min using an Easy-LC II Nano-HPLC system (Thermo-Fisher) containing a mixture of solvent A (3% ACN: 0.1% FA) and solvent B (99.9% ACN: 0.1% FA). Peptide quantification and analysis were carried out using Proteome Discoverer 2.2 (Thermo-Fisher), where the precursor ion tolerance used for peptide sequence matching was 10 ppm and 0.6 Da for fragment tolerance (Raheja et al. 2020).

Oxidative regioselectivity by high-resolution mass spectroscopy (HRMS) studies

For the HRMS studies, oxidative products released after the hydrolysis were analyzed using a Bruker micro TOF Q II Mass spectrometer (Bruker, Billerica, MA, USA) with 4500 V of capillary voltage, temperature of 180°C and working in ESI mode (+ve). Hydrolysis of substrates Avicel and CMC (2% w/v) was carried out by purified enzymes LPMO1 and LPMO2 for 96 h at 60°C in the presence of 1 mM ascorbate and 20 µM H_2O_2 (Agrawal et al. 2020a). For analysis,

the samples were prepared in acetonitrile with ratio of 3:7, respectively, and filtered using a 0.2 µM filter (PALL, New York, NY, USA) before being directly injected into the column. The mass/charge (m/z) ratio of the active peaks in the chromatogram was identified using the Bruker data analysis v 5.0 software (Bruker GmbH, Germany) and compared with the previously reported literature as reference (Isaksen et al. 2014).

Enzymatic hydrolysis and cocktail designing

The hydrolytic potential of both recombinant LPMOs was evaluated using acid/steam pretreated unwashed rice straw slurry procured from PRAJ Industries (Pune, India), a globally leading company involved in establishing of 2G ethanol demonstration plants in India and providing technical know-how internationally. For hydrolysis, a custom-designed cocktail was constituted by replacing the one part of cellulase preparations from bench mark enzyme (obtained from an in-house developed *R. emersonii* mutant M36 strain) with an enzyme loading rate of 5 mg/g dry substrate equivalent to ~100 µL with the auxiliary enzymes (LPMO1 and LPMO2) in 9:1 ratio, where the constituted cocktails contained benchmark cellulase (4.5 mg/gram dry substrate) produced by mutant M36 and 0.5 mg/gram dry substrate of either LPMO1/LPMO2. The performance of designed cocktail was compared with the cellulase blend CellicCtec3 (Novozymes, Bagsværd, Denmark; procured from PRAJ) at enzyme loading rate of 5 mg/gram dry substrate. A control cocktail, where the LPMO was replaced with a non-enzyme protein component, i.e., bovine serum albumin (BSA, 0.5 mg/gram dry substrate), was also included. The hydrolytic reaction setup in a total volume of 1 mL (carried out in a 15 mL glass vials) that contained 0.17 g (on dry weight basis) of the pretreated substrate slurry (pH 5.0) and the constituted enzyme cocktails (as mentioned above) were incubated for 72 h at 50°C, 200 rpm. The hydrolysis reactions were stopped by boiling for 10 min. After cooling, the reactions were suitably diluted using autoclaved distilled water, released glucose, and total reducing sugars were estimated. 3,5-dinitrosalicylic acid (DNS) based method was used for the determination of total reducing sugars, where 1 mL of the suitably diluted samples was mixed with 3 mL of DNS, followed by boiling for 10 min. The developed color was quantified at 540 nm (Miller 1959). The estimation of glucose was carried out using a GOD-POD kit (AUTOSPAN, Arkay Inc., Kanpur, India), with the reaction mixture comprising 1 mL of GOD-POD reagent and 50 µL of diluted sample. All reactions were incubated at 37°C for 10 min, and the developed color was read at 505 nm (Lin et al. 1999). Similar reactions were also carried out by the addition of 1 mM ascorbic acid and 20 µM H_2O_2 concentration. The detailed analysis of the end products formed in hydrolysate was carried out using Dionex 3000 ultimate HPLC fitted with an Aminex HPX 87H column (BioRad, Hercules, CA, USA) attached to Shodex RI 101 refractive index detector. For mobile phase, deionized water was used with adjusted flow rate of 0.6 mL/min and the column temperature maintained at 60°C. The resultant peaks were quantified based on the area and retention time of respective standards (Kaur et al. 2014).

Results

Cloning and expression of LPMO1 and LPMO2 in *P. pastoris*

The genes *LPMO1* (Talem1p7_017256) and *LPMO2* (Talem1p7_002983) possess open reading frames (ORF) of 765 bp and 1242 bp, respectively. The molecular weight of recombinant LPMO1 and LPMO2 was confirmed to be ~30 kDa and ~47 kDa, respectively (Fig. 1), which were higher than the masses computed using the Expasy tool (27.17 kDa for LPMO1 and 44.17 kDa for LPMO2 without signal peptide). The high molecular mass may be ascribed to the presence of *N*-glycosylation in both the LPMO1 and LPMO2 as predicted by online server NetNGlyc1.0 (http://www.cbs.dtu.dk/services/NetNGlyc/).

The colonies obtained after transformation were screened for the recombinant protein expression on the BMMY medium with 1% feeding rate of methanol at regular intervals of 24 h (Supplemental Fig. S1). The maximum expression of 670 and 500 units/L of activity was obtained for LPMO1 and LPMO2, respectively, using CMC as the substrate (Basotra et al. 2019). Furthermore, the specific activity of selected LPMO clones against 2,6-DMP substrate was found to be 32.46 and 14.32 units/g of enzyme for LPMO1 and LPMO2, respectively (Table 1).

Genome profiling of auxiliary activity enzymes in different thermophilic fungi, molecular modeling, and phylogenetic analysis of LPMO1 and LPMO2

The functional annotation of the *R. emersonii* genome (available at: https://genome.jgi.doe.gov/portal/) showed the presence of 58 genes that code for auxiliary activity (AA) enzymes. Among these, only 2 genes encode AA9 enzymes with lytic polysaccharide monooxygenase activity (LPMO1 and LPMO2). In contrast, the profiling of other thermophilic fungal genomes such as *Mycothermus thermophilus*, *Myceliophthora thermophila*, *Chaetomium thermophilum*, and *Malbranchea cinnamomea* showed a large subset of AA9s encoding 27, 23, 19, and 8 genes, respectively (Supplemental Fig. S2). The genome of *R. emersonii* was found to code for just one unidentified GMC oxidoreductase, while it did not contain any genes responsible for cellobiose

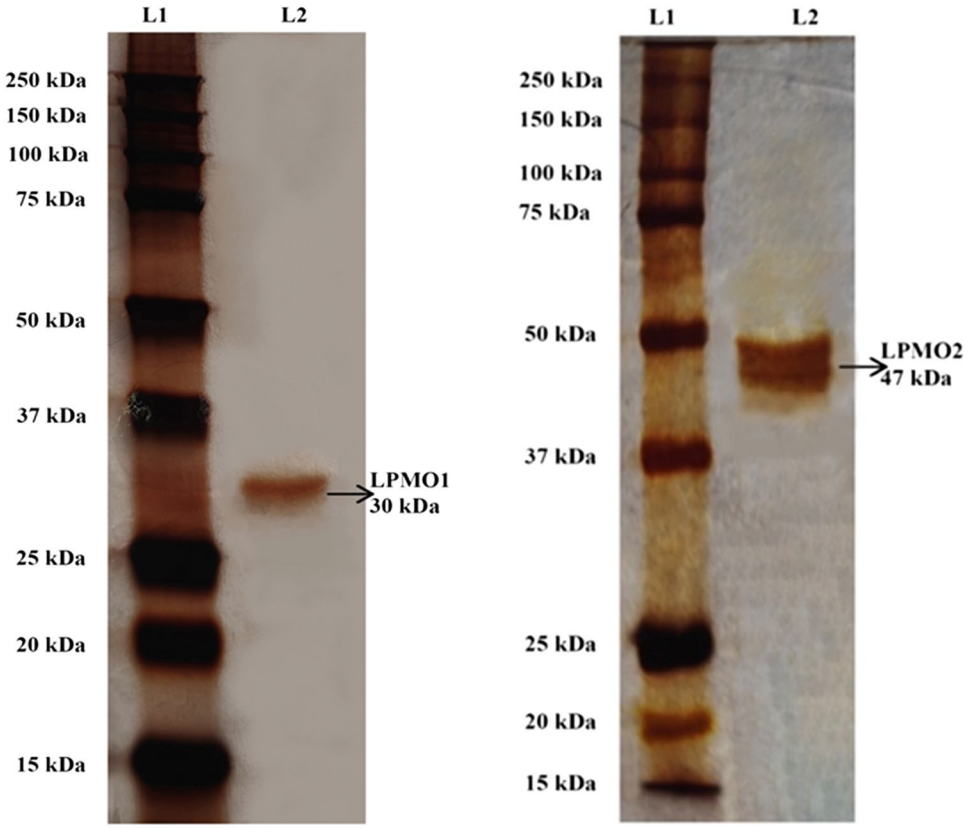

Fig. 1 SDS–PAGE analysis of purified LPMO1 and LPMO2. Lane L1: standard protein marker in kDa. Lane 2: purified LPMO1 (30 kDa) and LPMO2 (47 kDa), respectively

Table 1 Estimated activities of LPMO1 and LPMO2 assayed against different substrates

P. pastoris positive clones	Substrate used	Enzyme activity
LPMO1	CMC	670 units/L
	2,6 DMP	32.46 units/g of enzyme
LPMO2	CMC	500 units/L
	2,6 DMP	14.32 units/g of enzyme

CMC: carboxymethyl cellulose; 2,6 DMP: 2,6-dimethoxyphenol

dehydrogenase (CDH), which is known for its role as a reducing agent in LPMO-mediated catalytic process (Frommhagen et al. 2018). Furthermore, based on the multiple sequence alignment, LPMO1 showed high sequence similarity with *Penicillium verruculosum Pv*LPMO9A (75%) and *T. aurantiacus Ta*LPMO9A (78%) and LPMO2 showed 70.74, 41.86% similarity with C_1/C_4 specific LPMOs of *Aspergillus fumigatus* and *N. crassa*. The phylogenetic analysis clustered the LPMO1 with Type 3 LPMOs from *P. verruculosum* and *T. aurantiacus* as indicated by high bootstrap values, whereas, LPMO2 shared the same branch with the LPMOs of *Aspergillus ruber* and *A. fumigatus* (characterized as Type 3) (Fig. 2a). The phylogenetic analysis placed both LPMO1 and LPMO2 as Type 3 enzymes (Isaksen et al. 2014). These predictions were later validated by the mass spectrometry analysis. In silico studies were carried out by predicting the homology models and were checked for their quality by Ramachandran plot showing the presence of 97.5 and 95.52% residues in the allowed and favored regions, respectively, which suggests that the models are of good quality and reliable for structural analysis (Supplemental Fig. S3).

The 3D structures of LPMO1 and LPMO2 reveal a differential arrangement of the conserved catalytic residues present in the Cu-histidine brace. In LPMO1, the copper (Cu^{2+}) is coordinated by the two histidine residues, His1 and His86, at distances of 2.03 and 2.11 Å, respectively, and the axial position of the protein is occupied by the phenolic oxygen of the tyrosine (Tyr175) residue at a distance of 2.2 Å from Cu^{2+} (Fig. 2b). However, the conserved amino acids His1, His84, and Tyr168 constituted the histidine brace of LPMO2. To evaluate the structural basis of LPMO attack on crystalline cellulose (Avicel), molecular docking was carried out. As illustrated in Fig. 2c and d, glucosyl unit of the +1 subsite of Avicel (O_5 ring) is directly regulated by hydrogen bonding with the His1 centroid at 2.05 Å. O2 and O11 (subsite −1) of the substrate is directly arched over the N2 of Asn46 and the O atom of Gln31, respectively. Other residues held in the binding cavity of LPMO1 are

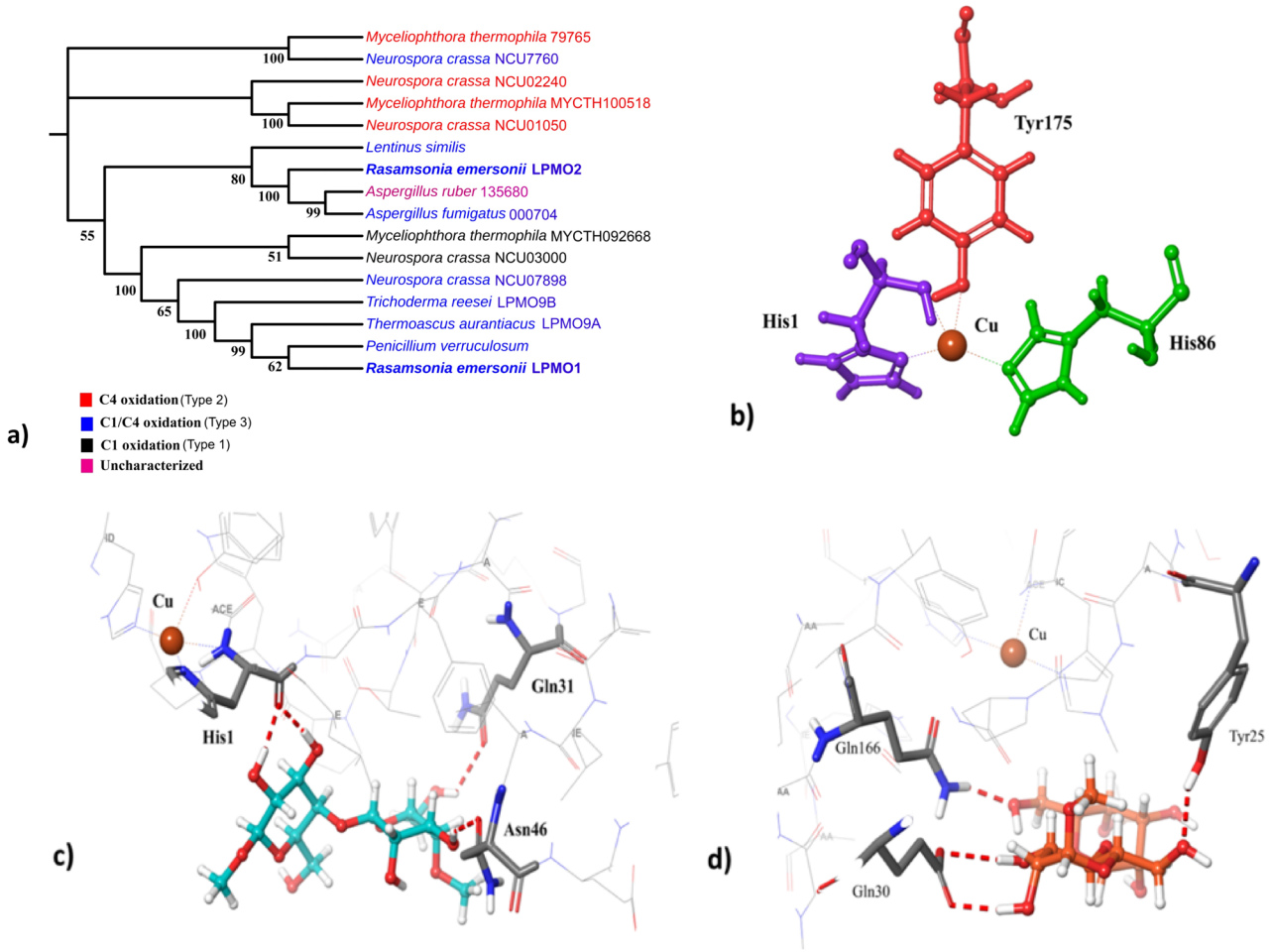

Fig. 2 In silico analysis of LPMOs. Representation of **a** phylogenetic tree of LPMOs from *R. emersonii* categorized on the basis of regioselectivity: Type 1 (C_1 oxidizing), Type 2 (C_4 oxidizing), and Type 3 (C_1/C_4 oxidizing); **b** conserved catalytic core of Cu histidine brace; **c** docking of LPMO1 with Avicel substrate, and **d** docking of LPMO2 with Avicel substrate

Pro83, Pro107, Trp105, and Thr 106 (Fig. 2c). Upon binding of Avicel on the surface of LPMO2, CH_2OH group of the +1 glucosyl subunit is bound to the O atom of Gln166 (1.98Å) and the −1 subunit is bound to Tyr25 (2.06Å) and Gln30 (2.24Å) via hydrogen bonding (Fig. 2d). Other amino acid residues formulating the binding site are Pro81, Pro43, His84, Ile29, His157, His1, and Gly27. The MMGBSA calculations for the ligand-binding affinities for LPMO1 and LPMO2 were −34.20 and −26.58 kcal/mol, respectively, indicating a higher binding affinity of LPMO1 to the crystalline cellulose.

Characteristics of purified LPMO1 and LPMO2

The expressed proteins of the selected recombinant LPMO clones were purified using single step anion exchange chromatography, using UNOSPHERE Q (Bio-Rad, Hercules, CA, USA). The purified LPMO1 and LPMO2 were found to be optimally active under alkaline conditions, with LPMO1 exhibiting maximal relative activity (119%) at pH 9.0 and LPMO2 showing 121% relative activity at pH 8.0 (Fig. 3a). Interestingly, these LPMOs also registered a relative activity of 80% at pH 5.0. Both LPMOs were optimally active at 60°C, beyond of which a marked decline in enzymatic activity was observed (Fig. 3b).

Furthermore, it was observed that the purified LPMO1 showed high stability of $t_{1/2}$ = ~71 h at pH 7.0; $t_{1/2}$ = ~80 h at pH 9.0 at 50°C in comparison to $t_{1/2}$ = ~24 h at pH 7.0, and $t_{1/2}$ = ~48 h at pH 9.0 at 60°C (Fig. 3c). Similarly, purified LPMO2 exhibited $t_{1/2}$ of ~96 h at pH 7.0 and $t_{1/2}$ of ~120 h at pH 8.0 in comparison to $t_{1/2}$ = ~72 h at pH 8.0, and $t_{1/2}$ = ~24 h at pH 7.0 at 60°C (Fig. 3d). The catalytic efficiency (k_{cat}/K_m) of purified LPMO1 and LPMO2 studied using Avicel as substrate was observed to be 6.6×10^{-2} mg^{-1} ml min^{-1} and 1.8×10^{-2} mg^{-1} ml min^{-1}, respectively. The purified LPMO1 and LPMO2 showed 1.18

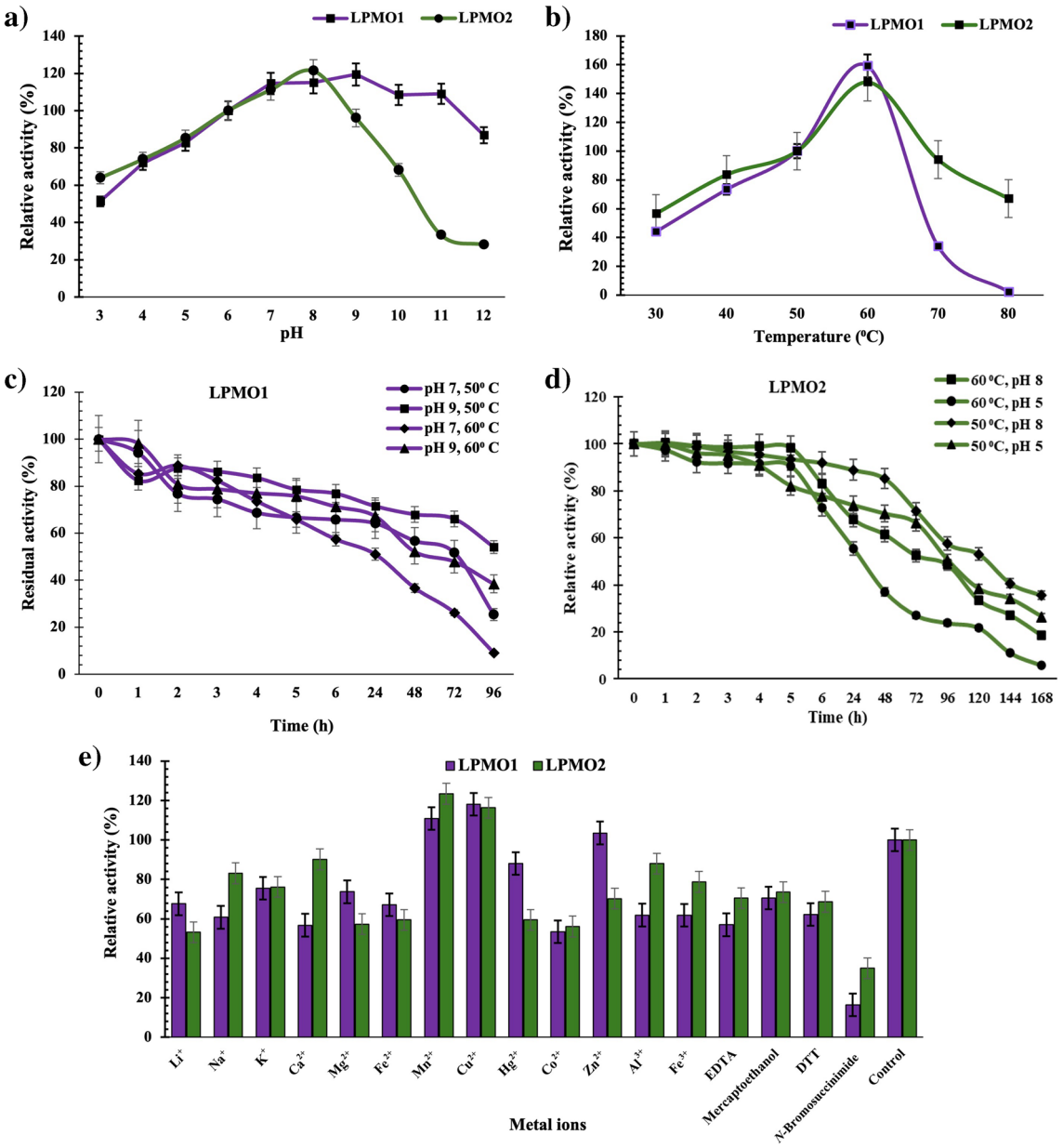

Fig. 3 Graphs showing **a** effect of pH (3.0–12.0) on the relative activity of LPMO1 and LPMO2 profiled against 2% CMC in the presence of 1 mM ascorbic acid (reducing agent) at 50°C, **b** the effect of temperature (between 20 and 80°C) on the activity of LPMO1 and LPMO2, **c** and **d** thermostability studies for LPMO1 (pH 7.0 and 9.0 and temperatures 50°C and 60°C) and LPMO2 (pH 7.0 and 8.0; temperatures 50°C and 60°C), **e** the effect of metal ions (5 mM) by incubating LPMO1 and LPMO2 for 30 min at room temperature on the activity of LPMO1 and LPMO2 using 2% CMC in the presence of 1 mM ascorbic acid (reducing agent). Relative significantly different values are * marked. Values represent mean ± SE (n=3). EDTA, ethylenediamine tetraacetic acid; DTT, Dithiothreitol

and 1.16-fold enhancement in activity when pre-incubated with Cu^{2+}, respectively (Fig. 3e). In addition, Mn^{2+} has been found to positively modulate the relative activity of LPMO1 and LPMO2 by 110 and 123%, respectively. Previously, PMO9A_MALCI (*M. cinnamomea*) also showed enhanced activity when pre-incubated with Cu^{2+} (127 %) and Mn^{2+} (117 %) metal ions; similarly, the activity of PMO9D_SCYTH (*Scytalidium thermophilum*) was found to be positively upmodulated in presence of Mn^{2+} (157 %) (Basotra et al. 2019; Agrawal et al. 2020a).

Both the purified LPMOs were active against different cellulosic and mixed linkage glucans with LPMO1 having high catalytic preference toward CMC (17.68 U/mg) followed by barley β glucan (15.36 U/mg), lichenan (10.62 U/mg) and Avicel (1.42 U/mg). However, the highest specific activity of LPMO2 was obtained against barley β

glucan (7.6 U/mg) followed by lichenan (5.29 U/mg), CMC (4.25 U/mg), and Avicel (0.53 U/mg) (Fig. 4a). No activity was detected against laminarin, starch, and xylan.

The role of H_2O_2 as co-substrate was studied on LPMO1 and LPMO2 activity. The results showed that the activity of LPMO1 and LPMO2 was upmodulated by 1.83 and 1.70 folds, respectively, in the presence of 20 µM H_2O_2 and 1 mM ascorbic acid (Fig. 4b). Moreover, the mass spectrometry examination of the hydrolysed mixture incubated with CMC and Avicel verified the release of both oxidized and non-oxidized compounds, along with cello-oligosaccharides ranging from degree of polymerization DP2 to DP8. This observation suggests the generation of aldonic acid and gemdiol at the C_1 and C_4 positions (Supplemental Fig. S4), respectively, indicating that both LPMO1 and LPMO2 fall within the category of Type 3 LPMOs (Isaksen et al. 2014).

Gene expression analysis of LPMOs on different carbon sources

Time scale dependent transcriptional profiling of *LPMO1* and *LPMO2* from *R. emersonii* was carried out upto 9 days of incubation. The results showed that the transcript levels of *LPMO1* (Talem1p7_017256) were up-regulated by 562-fold after 3 days of culturing on a medium that contained cellulose and chick pea as carbon sources (Fig. 5). The expression levels started decreasing thereafter to attain 298-fold by day 9 of culturing. Whereas, maximal expression (6.91 folds) of *LPMO2* (Talem1p7_002983) was observed after 5 days of incubation. The observed expression of *LPMO1* was 82-fold higher when compared to *LPMO2* and thus was designated as the major and minor LPMOs, respectively.

Although the genome of fungal strains harbor multiple genes for LPMOs, however, the knowledge about how they are expressed when fungal strains are cultured in medium containing different carbon (monomeric, oligomeric, and polymeric form) remains obscure. Therefore, the present study examined the differential expression of two LPMOs (annotated in *R. emersonii* genome), by culturing the strain in presence of different combinations of carbon sources. It was observed that addition of 1% glucose to the cellulose-based medium resulted in 1.4 folds higher expression of *LPMO1* gene when compared to cellulose-based medium after 3 days of incubation. However, in the presence of crystalline Avicel, the maximal expression of *LPMO1* (observed after 5 days of incubation) was ~25% less when compared to cellulose-based medium (Fig. 5c). Likewise, maximal expression of *LPMO2* was observed in the presence of Avicel after 5 days of incubation; however, the expression levels were ~45 folds lower when compared to expression of *LPMO1* in presence of Avicel (Fig. 5d). The medium that contained endoglucanase hydrolysed acid pretreated rice straw slurry from PRAJ [D(oligo EG)] that primarily comprised of cello-oligosaccharides, resulted in severe repression in the expression of *LPMO1*. However, the repression observed in presence of steam/acid pretreated rice straw slurry as a substrate was comparatively less severe even though the pretreated slurry contains the monomeric sugars xylose and glucose as well as inhibitors like acetic acid, hydroxy methyl furfural, and furfurals as analyzed by HPLC (Supplemental Table S4).

Differential proteome-based profiling of LPMOs and other auxiliary, glycosyl hydrolase enzymes grown on different substrates

The proteomic analysis of culture extracts grown in the presence of different carbon sources was evaluated

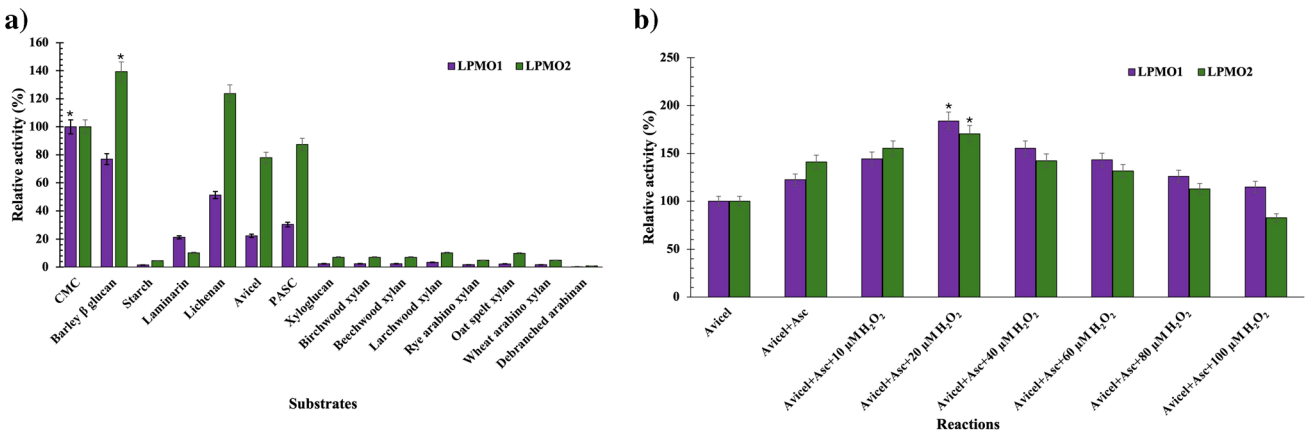

Fig. 4 Graphs showing **a** the substrate specificities at concentrations of 2% (w/v) for each substrate prepared in 50 mM Tris chloride buffer at pH 9.0 for LPMO1 and pH 8.0 for LPMO2 at 60°C for 2 h, and **b** the effect of H_2O_2 (concentrations 10–100 µM) addition on the activity of LPMO1 and LPMO2 assayed against 2% w/v Avicel. *Relative significantly different values detected in the experiment. Bars represent mean ± SE (n=3). "Asc" refers to the ascorbic acid

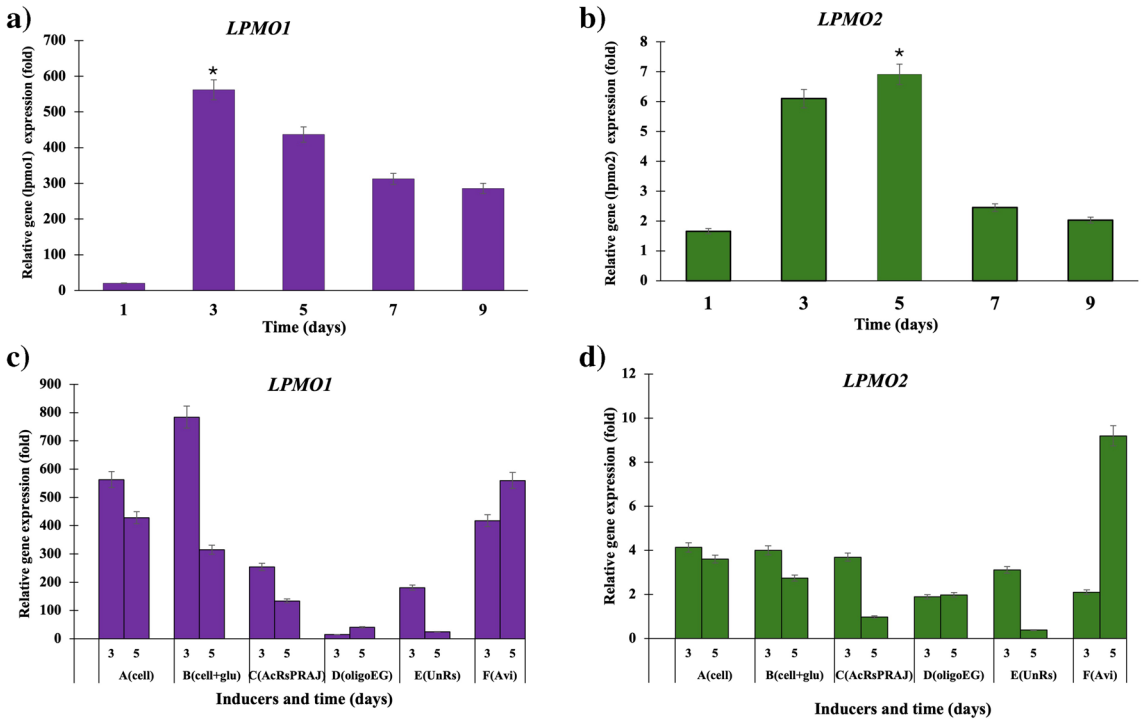

Fig. 5 Real-time RT-PCR based temporal gene expression analysis of **a** *LPMO1* and **b** *LPMO2* transcripts and gene expression profiling of **c** *LPMO1* **d** *LPMO2* transcripts on 3rd and 5th day under different carbon sources. A(cell) = cellulose; B(cell+glu) = cellulose+glucose; C(AcRsPRAJ) = acid pre-treated rice straw slurry; D(oligoEG) = endoglucanase hydrolysed rice straw slurry; E(UnRs) = untreated rice straw; F(Avi) = Avicel. * indicates the maximum expression of genes

(data submitted with ProteomeXchange Consortium via the PRIDE partner repository; Project Accession no. PXD046292 and Project https://doi.org/10.6019/PXD046292). The CAZyme profiling of the culture extract grown in the presence of cellulose supplemented with glucose constituted 5.5% of auxiliary activity proteins of the total secretome (Supplemental Fig. S5). However, it was observed that the level of expressed LPMO1 (AA9) was only 2.84%. The observed levels of expressed LPMO1 in presence of amorphous cellulose and Avicel were found to be 1.83% and 0.56%, respectively. Whereas in the presence of endoglucanase hydrolysed acid pretreated rice straw slurry (PRAJ [D(oligo EG)]) rich in oligosaccharides, a severe repression in LPMO1 (0.08%) levels was observed. Although LPMO2 expression was detected at transcriptional level but none of the analyzed secretome derived from different media types (Table 2) showed its expression, which may be attributed to multiple levels of hierarchal determinants such as the presence of a suitable inducer that trigger the *cis*-acting transcriptional factors regulating the gene expression and eventually participating in the coordinated protein production. The ultimate fate of protein secretion is governed by translation, ER (endoplasmic reticulum) mediated folding followed by glycosylation in Golgi and transmembrane trafficking (Yan et al. 2021).

The observed negative effect of oligosaccharides at transcriptional and translational levels on the expression of LPMOs in this study are being reported for the first time. Interestingly, when compared to other media types, maximal expression of laccase AA1_3 corresponding to 1.58% and 1.40% was observed in medium containing steam/acid pretreated rice straw slurry and endoglucanase hydrolysed oligosaccharide rich slurry, respectively. The culture medium containing untreated rice straw, however, showed maximal expression of AA7 oxidoreductase (1.93%) followed by oligosaccharide rich endoglucanase treated rice straw slurry (0.99%) (Table 2). Moreover, catalase and superoxide dismutase enzymes represented 0.21% and 1.32%, of the secreted proteins in the culture medium comprising of cellulose and glucose, respectively.

Hydrolytic potential of LPMOs and cocktail designing

The results in Fig 6a and b, show that the cocktail developed by replacing one part of lignocellulolytic preparation (composition mentioned in Supplemental Table S2) of *R. emersonii* mutant M36 strain with those from recombinant clones LPMO1 and LPMO2 (9:1) improved the hydrolysis of steam/acid pretreated unwashed rice straw slurry (procured from PRAJ; composition of substrate mentioned in

Table 2 Comparative profiling of auxiliary and cellulase enzymes in the secretome of *R. emersonii*

Protein	Accession no.	Family	A(cell)	B (cell+glu)	C(AcRsPRAJ)	D (oligoEG)	E (UnRs)	F (Avi)
Auxiliary enzymes								
LPMO1	Talem1p7_017256	AA9	1.83	2.84P	0.29	0.08	0.040	0.56
LPMO2	Talem1p7_002983	AA9	-	-	-	-	-	-
Laccase abr2	Talem1p7_016942	AA1_3 - AA1_1	0.79	0.80	1.58	1.40	0.62	1.46
Iron transport multicopper oxidase fetC	Talem1p7_010576	AA1_2	0.004	0.016	0.01	0.03	0.06	0.01
Glucose oxidase	Talem1p7_010453	AA3_2	0.010	0.015	0.06	0.29	0.11	0.01
Dehydrogenase citC	Talem1p7_015022	AA3_2	0.119	0.114	-	-	0.04	-
Alcohol oxidase 1	Talem1p7_002247	AA3_3	0.021	0.015	-	-	-	0.08
Oxygen-dependent choline dehydrogenase	Talem1p7_016253	AA3	0.015	0.012	-	-	-	-
Protoplast-secreted protein 2	Talem1p7_002425	AA6	0.022	0.024	-	-	-	-
FAD-linked oxidoreductase chyH	Talem1p7_016255	AA7	0.22	0.30	0.22	0.99	1.93	0.18
FAD-linked oxidoreductase afoF	Talem1p7_002172	AA7	0.42	0.47	0.01	0.02	0.03	0.01
FAD-linked oxidoreductase ARB_02478	Talem1p7_006075	AA7	0.38	0.59	0.17	0.12	-	0.26
FAD-linked oxidoreductase ARB_02372	Talem1p7_008090	AA7	0.01	0.005	0.02	0.03	0.03	0.01
6-hydroxy-D-nicotine oxidase	Talem1p7_006672	AA7	0.09	0.10	-	-	-	-
FAD-dependent monooxygenase yanF	Talem1p7_018326	AA7	0.06	0.02	0.09	0.03	0.07	0.10
Hypothetical protein	Talem1p7_017049	AA11	0.22	0.18	0.15	0.16	0.15	0.10
Total			4.211	5.501	2.60	3.15	3.08	2.78
Other enzymes								
Catalase	Talem1p7_004750	-	0.12	0.21	-	-	-	-
Superoxide dismutase	Talem1p7_009715	-	1.00	1.32	0.02	0.02	0.02	0.02

A(cell), cellulose; *B(cell+glu)*, cellulose+glucose; *C(AcRsPRAJ)*, acid pre-treated rice straw slurry; *D(oligoEG)*, endoglucanase hydrolysed rice straw slurry; *E(UnRs)*, untreated rice straw; *F(Avi)*, Avicel

Here "–" indicates protein not detected in the secretome

(Project Accession no. PXD046292; Project PDOI: 10.6019/PXD046292)

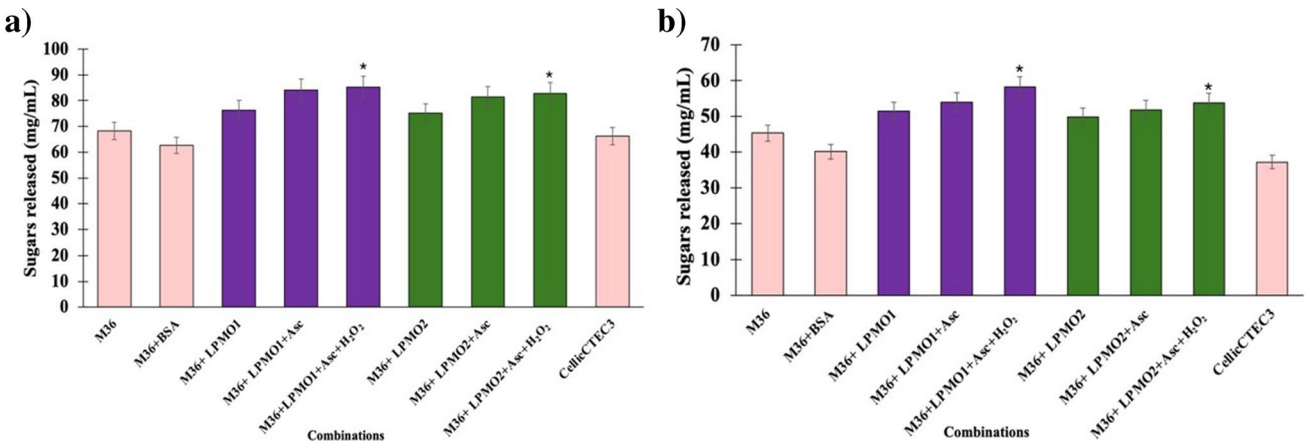

Fig. 6 Graph showing **a** amount of released total reducing sugars and **b** glucose after hydrolysis of steam/acid pretreated unwashed rice straw slurry procured from PRAJ industry Ltd. for 72 h at 50°C, 200 rpm. Bars represent mean ± SE (n=3). * indicates the maximum release of total reducing sugars and glucose. "Asc" refers to the ascorbic acid

Supplemental Table S4). The observed saccharification efficacy of in-house cellulolytic preparation of *R. emersonii* M36 was 73.89% that was enhanced to 87.94 and 85.46%, when cocktails comprising of LPMO1 and LPMO2 were constituted, respectively (Fig. 6).

The hydrolytic performance of the cocktails was also found to be superior when compared to commercial cellulase CellicCtec3, where 68.26% saccharification efficiency was observed at the same enzyme loading rate. The results indicates that the addition of LPMO1 and LPMO2 to the in-house developed crude cellulase mix resulted in 19.01%, 15.66% increase in the total reducing sugar yield and 28.57%, 18.81% in glucose release, respectively, when compared to the control. This study on the basis of the comparative analysis of LPMOs (Supplemental Table S3) shows that both the major expressed LPMO1 (major) and LPMO2 (minor) have an important role in formulating the biorefinery relevant enzyme cocktails capable of hydrolysing at high substrate loading rate.

Discussion

The current work reports the cloning and expression of 2 LPMO genes (AA9 family) from *R. emersonii* utilizing the expression host *P. pastoris* X-33 to define and compare the catalytic efficiency of recombinant enzymes. To the best of our knowledge, detailed functional analysis of LPMOs (AA9 family) from *R. emersonii* has not been reported previously. Since enzymes belonging to AA9 family were originally categorized as GH61 that exhibited weak endoglucanase activity against CMC as substrate, therefore, in the present study the LPMO activity was assayed against CMC as a substrate as well as recently reported method for enzyme assay using 2,6-DMP as a substrate, that relies on LPMO-mediated formation of coerulignone, was also included (Breslmayr et al. 2018). The LPMO1 and LPMO2 showed specific activity of 32.46 and 14.32 U/g, respectively, against 2,6-DMP as substrate (Table 1). The estimated titres of LPMO activity assayed against 2,6 DMP were higher when compared to LPMO9F (2.2 U/g) expressed in *N. crassa* (Breslmayr et al. 2018).

The physicochemical features of both the LPMOs, evaluated at different pH levels, indicated that 80% of the activity was retained at pH 5.0, indicating its relevance in the hydrolysis of lignocellulosic biomass, which is typically carried out at acidic pH values of 4.5-5.0 (Baig 2020). The existing commercial enzyme blends that are derived from the mesophilic strains of *Trichoderma reesei*, *Penicillium decumbens*, and *Acremonium cellulolyticus* are catalytically less efficient, and therefore, thermophilic fungal strains such as *T. aurantiacus*, *M. thermophila* are preferred these days due to the high thermostability and rate of catalysis (Adsul et al. 2020). The findings of the present study revealed that the optimal temperature for enzymatic activity of both purified LPMOs was 60°C, and their higher thermostability renders them as preferable choice for lignocellulosic hydrolysis. Previous research has also highlighted the advantages of utilizing LPMOs with high thermostability, which holds immense potential for acid and alkali pretreated substrates in 2G ethanol biorefineries (Agrawal et al. 2020a). The fact that Cu^{2+} is an integral part of copper containing LPMO, where it acts as co-factor in oxidative cleavage, both the LPMOs showed elevated activities when pre-incubated with Cu^{2+}. Previously, PMO9A_MALCI from *M. cinnamomea* also showed enhanced activity when pre-incubated with Cu^{2+} (127%), similarly Mn^{2+} (117%) that has also been shown to positively modulate PMO9D_SCYTH from *S. thermophilum* activity by 157% (Basotra et al. 2019; Agrawal et al. 2020a). The addition of Mn^{2+} in the reaction mixture for mediating LPMO-driven disintegration of cellulosics has also been experimented previously (Harris et al. 2010). The LPMOs in present study showed high substrate specificity for glucan-based polymers, CMC, barley β-glucan, lichenan, and Avicel and were found to preferentially cleave (1→4/1→3) β-D glucan backbone. Similarly, LPMOs from *Lentinus similis* and *Collariella virescens* also showed an akin cleavage pattern against the (1→4) β-D glucan backbone substrates (Simmons et al. 2017). The recent past studies have reported that H_2O_2 instead of O_2 act as a co-substrate for supporting LPMO-mediated catalytic reaction (Bissaro et al. 2017, 2018; Zhang et al. 2021b). ScLPMO10C, from the actinomycete *Streptomyces coelicolor*, is shown to abstract oxygen from H_2O_2 (200 µM), which has been recognized as a co-substrate, and introduces a nick at the C_1 or C_4 position. This results in a 26-fold higher release of soluble products from chitin compared to the control without H_2O_2, indicating ScLPMO10C to be a peroxygenase (Bissaro et al. 2017). Whereas the effect of adding H_2O_2 (20 µM) as a co-substrate in *R. emersonii* was not that pronounced as only 1.83 and 1.70 folds, higher activity was observed in LPMO1 and LPMO2, respectively. A similar effect of H_2O_2 addition on the activity of LPMOs from other thermophilic and thermotolerant strains, i.e., PMO9D_SCYTH (*S. thermophilum*; 60 µM), PMO9D_MALCI (*M. cinnamomea*; 40 µM) PMO_08942, PMO_07920 (*Aspergillus terreus*; 40 µM) (Agrawal et al. 2020a, b a, b) was reported from our lab previously, where the up-modulation of LPMO activity by 1.6 to 7.04 folds in presence of H_2O_2 was observed.

Although the LPMOs are known to degrade the lignocellulosic biomass, how their expression is controlled by complex carbon sources during enzyme production is unknown. Therefore, the temporal and differential expression of both the LPMOs was examined on a range of polysaccharides based complex culture media types. In the present work, maximal expression of *LPMO1* was observed after 3 days

of incubation on an amorphous cellulose-based medium, whereas expression of *LPMO2* peaked after 5 days of incubation on Avicel (crystalline cellulose)–based medium. In a recent report that compared the temporal expression of different LPMOs from the thermophilic fungus *C. thermophilum*, maximal induction of LPMOs was also found after 5 days of incubation when cultured on microcrystalline cellulose (MCC) based medium (Li et al. 2020). Transcriptional profiling in the presence of different carbon sources indicated the downregulation of LPMO1 in presence of oligosaccharides in the medium D [(oligo EG)] that are obtained by controlled hydrolysis of acid/steam pretreated rice straw slurry by mono-component endoglucanase (GH5) from *R. emersonii*. However, a less severe impact was observed in the steam/acid-pretreated slurry based medium, which contains monomeric sugars such as xylose and glucose, as well as hydrolytic inhibitors. The negative impact of monomeric sugars (glucose) on the expression of 5 different LPMOs in *Thielavia terrestris* (Tõlgo et al. 2021) has been shown; however, our study clearly suggests a much more pronounced negative impact of cello-oligosaccharides on the expression of LPMOs.

Furthermore, the quantification of both the LPMOs and their interplay with other classes of auxiliary enzymes was examined using proteome-based analysis. The results showed that only LPMO1 was expressed to detectable levels in the secretome; however, the LPMO2 remained unexpressed (or undetected) in all the media types studied. Addition of glucose as a carbon source supported the expression of *T. aurantiacus* LPMO_39370 and other classes of auxiliary enzymes in comparison to cellulose, arabinose, and xylose as the inducers (Gabriel et al. 2021). Similarly, in the present study, the observed expression of LPMO1 protein was comparatively higher (2.42% of the total expressed protein) in medium that contained glucose and cellulose when compared to 1.65% in presence of cellulose which was coherent with the observed gene expression at transcriptional level. Interestingly, secretome profiling indicated that CDH was absent in the culture extracts, known to be an important cognate protein for donating electrons to the divalent copper present at the active site of LPMO, indicating the involvement of other redox partners in catalysis. The secretome data showed the presence of AA3_2 family of proteins, which are known to indirectly mediate the reduction of LPMOs by transferring the electrons to the active site of LPMOs, thereby playing a crucial role in the activation of LPMOs (Berrin et al. 2017). The co-secretion of AA3_2 and LPMOs (AA9) has been also been reported in the secretome of white rot fungus *P. cinnabarinus* (Miyauchi et al. 2020). Additionally, high expression of laccase AA1_3 in the medium containing acid pretreated slurry and endoglucanase treated slurry (Table 2) indicates to the role of laccases in the opening and realignment of the intricate lignocellulosic structure, thus exposing lignin. Significant expression of catalase and superoxide dismutase in the secretome derived from cellulose and glucose grown culture supports the possible role of superoxide dismutase in the generation of H_2O_2 that supports LPMO-mediated catalysis (Bissaro et al. 2017). In addition, it provides protection against the oxidative stress caused by the reactive oxygen species generated during mitochondrial electron transport, thereby preventing the inactivation of LPMOs and other cellulases (Frommhagen et al. 2018). On the other hand, catalase is involved in attenuating the level of H_2O_2 to prevent the denaturation of enzyme and the catalytic action of LPMO. The spiking of catalase into the commercial cellulase mixture has been reported to result in significant enhancement of saccharification efficiency and increase the stability of AA9 proteins (Scott et al. 2016). Furthermore, the efficacy of these heterologously expressed LPMOs was tested against steam/acid pretreated rice straw slurry procured from PRAJ Industries. The results showed that the addition of LPMO1 and LPMO2 to the in-house developed crude cellulase mix resulted in enhanced release of total reducing sugars and glucose yield. The addition of LPMOs to the base mixture of cellulase from *Penicillium funiculosum* and *T. terrestris* has been reported to result in 13% enhancement of saccharification of pretreated wheat straw and corn stover, respectively (Harris et al. 2010; Ogunyewo et al. 2020). The findings from this study show that both the major expressed LPMO1 as well as the minor LPMO2 that remains unrepresented in the secretome can play an important role in significantly enhancing the saccharification of acid steam pretreated lignocellulosics and can be considered as an important enzyme candidate for lignocellulolytic cocktail formulations. In conclusion, this study presents a comprehensive analysis of the transcriptional expression, catalytic activity, redox interplay with auxiliary enzymes, and 3D structure of two LPMO genes (LPMO1 and LPMO2) from *R. emersonii*. Overall, the results of this study provide valuable insights into the use of LPMOs in improving the saccharification of lignocellulosic substrates in 2G ethanol biorefineries.

Supplementary Information The online version contains supplementary material available at https://doi.org/10.1007/s00253-024-13240-0.

Acknowledgements Research projects "Novel concepts for developing efficient cellulolytic cocktail for hydrolysis of bio-refinery relevant pretreated lignocellulosics" [BT/PR31115/PBD/26/766/2019] by the Department of Biotechnology and the pretreated lignocellulosics materials supplied by PRAJ and IOCL are duly acknowledged.

Author contribution YR involved in conceptualization, performed experiments, analyzed data, and wrote the manuscript. VS was involved in methodology and data analysis. DA was involved in editing and review the manuscript. GS contributed analytical tools and review the manuscript. NK involved in software and data validation. AT and

MDF performed data curation and validation. BSC involved in project administration, resources, supervision, writing—review and editing. All authors read and approved the manuscript.

Data availability All data generated and analyzed during this study are included in this published article and its supplementary information files with secretome data available at PRIDE Proteomics Identification database (Accession no. PXD046292; https://doi.org/10.6019/PXD046292).

Declarations

Ethical approval This article does not contain any studies with human participants or animals performed by any of the authors.

Conflict of interest The authors declare no competing interests.

References

Adsul M, Sandhu SK, Singhania RR, Gupta R, Puri SK, Mathur A (2020) Designing a cellulolytic enzyme cocktail for the efficient and economical conversion of lignocellulosic biomass to biofuels. Enzyme Microb Technol 133:109442. https://doi.org/10.1016/J.ENZMICTEC.2019.109442

Agrawal D, Basotra N, Balan V, Tsang A, Chadha BS (2020a) Discovery and expression of thermostable LPMOs from thermophilic fungi for producing efficient lignocellulolytic enzyme cocktails. Appl Biochem Biotechnol 191:463–481. https://doi.org/10.1007/s12010-019-03198-5

Agrawal D, Kaur B, Brar KK, Chadha BS (2020b) An innovative approach of priming lignocellulosics with lytic polysaccharide mono-oxygenases prior to saccharification with glycosyl hydrolases can economize second generation ethanol process. Bioresour Technol 308:123257. https://doi.org/10.1016/j.biortech.2020.123257

Baig KS (2020) Interaction of enzymes with lignocellulosic materials: causes, mechanism and influencing factors. Biores Bioproc 7:1–9

Basotra N, Dhiman SS, Agrawal D, Sani RK, Tsang A, Chadha BS (2019) Characterization of a novel lytic polysaccharide monooxygenase from *Malbranchea cinnamomea* exhibiting dual catalytic behavior. Carbohydr Res 478:46–53. https://doi.org/10.1016/J.CARRES.2019.04.006

Berrin JG, Rosso MN, Abou Hachem M (2017) Fungal secretomics to probe the biological functions of lytic polysaccharide monooxygenases. Carbohydr Res 448:155–160. https://doi.org/10.1016/j.carres.2017.05.010

Bertini L, Breglia R, Lambrughi M, Fantucci P, De Gioia L, Borsari M, Sola M, Bortolotti CA, Bruschi M (2018) Catalytic mechanism of fungal lytic polysaccharide monooxygenases investigated by first-principles calculations. Inorg Chem 57:86–97. https://doi.org/10.1021/acs.inorgchem.7b02005

Bissaro B, Røhr ÅK, Müller G, Chylenski P, Skaugen M, Forsberg Z, Horn SJ, Vaaje-Kolstad G, Eijsink VGH (2017) Oxidative cleavage of polysaccharides by monocopper enzymes depends on H_2O_2. Nat Chem Biol 13:1123–1128. https://doi.org/10.1038/nchembio.2470

Bissaro B, Várnai A, Røhr ÅK, Eijsink VGH (2018) Oxidoreductases and reactive oxygen species in conversion of lignocellulosic biomass. Microbiol Mol Biol Rev 82:10–1128. https://doi.org/10.1128/mmbr.00029-18

Breslmayr E, Hanžek M, Hanrahan A, Leitner C, Kittl R, Šantek B, Oostenbrink C, Ludwig R (2018) A fast and sensitive activity assay for lytic polysaccharide monooxygenase. Biotechnol Biofuels 11:1–13. https://doi.org/10.1186/S13068-018-1063-6

Cavalaglio G, Gelosia M, Giannoni T, Barros Lovate Temporim R, Nicolini A, Cotana F, Bertini A (2021) Acid-catalyzed steam explosion for high enzymatic saccharification and low inhibitor release from lignocellulosic cardoon stalks. Biochem Eng J 174:108121. https://doi.org/10.1016/j.bej.2021.108121

Chylenski P, Bissaro B, Sørlie M, Røhr ÅK, Várnai A, Horn SJ, Eijsink VGH (2019) Lytic polysaccharide monooxygenases in enzymatic processing of lignocellulosic biomass. ACS Catal 9:4970–4991. https://doi.org/10.1021/acscatal.9b00246

Dadheech T, Jakhesara S, Chauhan PS, Pandit R, Hinsu A, Kunjadiya A, Rank D, Joshi C (2019) Draft genome analysis of lignocellulolytic enzymes producing *Aspergillus terreus* with structural insight of β-glucosidases through molecular docking approach. Int J Biol Macromol 125:181–190. https://doi.org/10.1016/j.ijbiomac.2018.12.020

Dessie W, Xin F, Zhang W, Zhou J, Wu H, Ma J, Jiang M (2019) Inhibitory effects of lignocellulose pretreatment degradation products (hydroxymethylfurfural and furfural) on succinic acid producing *Actinobacillus succinogenes*. Biochem Eng J 150:107263. https://doi.org/10.1016/j.bej.2019.107263

Frommhagen M, Westphal AH, van Berkel WJH, Kabel MA (2018) Distinct substrate specificities and electron-donating systems of fungal lytic polysaccharide monooxygenases. Front Microbiol 9:1080. https://doi.org/10.3389/fmicb.2018.01080

Gabriel R, Mueller R, Floerl L, Hopson C, Harth S, Schuerg T, Singer SW (2021) CAZymes from the thermophilic fungus Thermoascus aurantiacus are induced by C5 and C6 sugars. Biotechnology for biofuels 14:1–13. https://doi.org/10.1186/s13068-021-02018-5

Garajova S, Mathieu Y, Beccia MR, Bennati-Granier C, Biaso F, Fanuel M, Ropartz D, Guigliarelli B, Record E, Rogniaux H, Henrissat B, Berrin JG (2016) Single-domain flavoenzymes trigger lytic polysaccharide monooxygenases for oxidative degradation of cellulose. Sci Rep 6:1–9. https://doi.org/10.1038/srep28276

Harris PV, Welner D, McFarland KC, Re E, Navarro Poulsen JC, Brown K, Salbo R, Ding H, Vlasenko E, Merino S, Xu F, Cherry J, Larsen S, Lo Leggio L (2010) Stimulation of lignocellulosic biomass hydrolysis by proteins of glycoside hydrolase family 61: structure and function of a large, enigmatic family. Biochemistry 49:3305–3316. https://doi.org/10.1021/bi100009p

Hoda A, Tafaj M, Sallaku E (2021) In silico structural, functional and phylogenetic analyses of cellulase from *Ruminococcus albus*. J Genet Eng Biotechnol 19:1–5. https://doi.org/10.1186/s43141-021-00162-x

Hong J, Tamaki H, Kumagai H (2007) Cloning and functional expression of thermostable β-glucosidase gene from *Thermoascus aurantiacus*. Appl Microbiol Biotechnol 73:1331–1339. https://doi.org/10.1007/s00253-006-0618-9

Hoppert L, Kölling R, Einfalt D (2022) Synergistic effects of inhibitors and osmotic stress during high gravity bioethanol production from steam-exploded lignocellulosic feedstocks. Biocatal Agric Biotechnol 43:102414. https://doi.org/10.1016/J.BCAB.2022.102414

Horn SJ, Vaaje-Kolstad G, Westereng B, Eijsink VG (2012) Novel enzymes for the degradation of cellulose. Biotechnol Biofuels 5:45. https://doi.org/10.1186/1754-6834-5-45

Isaksen T, Westereng B, Aachmann FL, Agger JW, Kracher D, Kittl R, Ludwig R, Haltrich D, Eijsink VGH, Horn SJ (2014) A C4-oxidizing lytic polysaccharide monooxygenase cleaving both cellulose and cello-oligosaccharides. J Biol Chem 289:2632–2642. https://doi.org/10.1074/jbc.M113.530196

Jacobson MP, Pincus DL, Rapp CS, Day TJF, Honig B, Shaw DE, Friesner RA (2004) A hierarchical approach to all-atom protein loop prediction. Proteins: Struct Funct Bioinformat 55:351–367. https://doi.org/10.1002/prot.10613

Johansen KS (2016) Lytic polysaccharide monooxygenases: the microbial power tool for lignocellulose degradation. Trends Plant Sci 21:926–936. https://doi.org/10.1016/j.tplants.2016.07.012

Karlsson J, Saloheimo M, Siika-Aho M, Tenkanen M, Penttilä M, Tjerneld F (2001) Homologous expression and characterization of Cel61A (EG IV) of *Trichoderma reesei*. Eur J Biochem 268:6498–6507. https://doi.org/10.1046/j.0014-2956.2001.02605.x

Kaur B, Oberoi HS, Chadha BS (2014) Enhanced cellulase producing mutants developed from heterokaryotic *Aspergillus* strain. Bioresour Technol 156:100–107. https://doi.org/10.1016/j.biortech.2014.01.016

Kont R, Pihlajaniemi V, Borisova AS, Aro N, Marjamaa K, Loogen J, Büchs J, Eijsink VG, Kruus K, Väljamäe P (2019) The liquid fraction from hydrothermal pretreatment of wheat straw provides lytic polysaccharide monooxygenases with both electrons and H_2O_2 co-substrate. Biotechnol Biofuels 12:1–15. https://doi.org/10.1186/s13068-019-1578-5

Li X, Han C, Li W, Chen G, Wang L (2020) Insights into the cellulose degradation mechanism of the thermophilic fungus *Chaetomium thermophilum* based on integrated functional omics. Biotechnol Biofuels 13:1–18. https://doi.org/10.1186/s13068-020-01783-z

Lin J, Pillay B, Singh S (1999) Purification and biochemical characteristics of *β*-D-glucosidase from a thermophilic fungus, *Thermomyces lanuginosus*-SSBP. Biotechnol Appl Biochem 30:81–87. https://doi.org/10.1111/j.1470-8744.1999.tb01163.x

Lowry OH, Rosebrough NJ, Farr AL, Randall RJ (1951) Protein measurement with the folin phenol reagent. J Biol Chem 193:265–275. https://doi.org/10.1016/s0021-9258(19)52451-6

Ma L, Liu Z, Kong Z, Wang M, Li T, Zhu H, Wan Q, Liu D, Shen Q (2021) Functional characterization of a novel copper-dependent lytic polysaccharide monooxygenase TgAA11 from *Trichoderma guizhouense* NJAU 4742 in the oxidative degradation of chitin. Carbohydr Polym 258. https://doi.org/10.1016/j.carbpol.2021.117708

Manavalan T, Stepnov AA, Hegnar OA, Eijsink VG (2021) Sugar oxidoreductases and LPMOs–two sides of the same polysaccharide degradation story? Carbohydr Res 505:108350. https://doi.org/10.1016/j.carres.2021.108350

Mellitzer A, Weis R, Glieder A, Flicker K (2012) Expression of lignocellulolytic enzymes in *Pichia pastoris*. Microb Cell Fact 11:1–11. https://doi.org/10.1186/1475-2859-11-61

Miller GL (1959) Use of dinitrosalicylic acid reagent for determination of reducing sugar. Anal Chem 31:426–428. https://doi.org/10.1021/ac60147a030

Miyauchi S, Hage H, Drula E, Lesage-Meessen L, Berrin JG, Navarro D, Rosso MN (2020) Conserved white-rot enzymatic mechanism for wood decay in the Basidiomycota genus Pycnoporus. DNA res 27(2):dsaa011. https://doi.org/10.1093/dnares/dsaa011

Momeni MH, Fredslund F, Bissaro B, Raji O, Vuong TV, Meier S, Nielsen TS, Lombard V, Guigliarelli B, Biaso F, Haon M, Grisel S, Henrissat B, Welner DH, Master ER, Berrin JG, Abou Hachem M (2021) Discovery of fungal oligosaccharide-oxidising flavoenzymes with previously unknown substrates, redox-activity profiles and interplay with LPMOs. Nat Commun 12:2132. https://doi.org/10.1038/s41467-021-22372-0

Müller G, Chylenski P, Bissaro B, Eijsink VGH, Horn SJ (2018) The impact of hydrogen peroxide supply on LPMO activity and overall saccharification efficiency of a commercial cellulase cocktail. Biotechnol Biofuels 11:1–17. https://doi.org/10.1186/s13068-018-1199-4

Ogunyewo OA, Randhawa A, Gupta M, Kaladhar VC, Verma PK, Yazdani SS (2020) Insights into structure of *Penicillium funiculosum* LPMO and its synergistic saccharification performance with CBH1 on high substrate loading upon simultaneous overexpression. bioRxiv 2020–04. https://doi.org/10.1101/2020.04.16.045914

Østby H, Hansen LD, Horn SJ, Eijsink VGH, Várnai A (2020) Enzymatic processing of lignocellulosic biomass: principles, recent advances and perspectives. J Ind Microbiol Biotechnol 47:623–657. https://doi.org/10.1007/S10295-020-02301-8

Pramanik SK, Mahmud S, Paul GK, Jabin T, Naher K, Uddin MS, Zaman S, Saleh MA (2021) Fermentation optimization of cellulase production from sugarcane bagasse by *Bacillus pseudomycoides* and molecular modeling study of cellulase. Curr Res Microb Sci 2:100013. https://doi.org/10.1016/j.crmicr.2020.100013

Raheja Y, Kaur B, Falco M, Tsang A, Chadha BS (2020) Secretome analysis of *Talaromyces emersonii* reveals distinct CAZymes profile and enhanced cellulase production through response surface methodology. Ind Crops Prod 152:112554. https://doi.org/10.1016/j.indcrop.2020.112554

Raheja Y, Singh V, Kaur B, Basotra N, Di Falco M, Tsang A, Singh Chadha B (2022) Combination of system biology and classical approaches for developing biorefinery relevant lignocellulolytic *Rasamsonia emersonii* strain. Bioresour Technol 351. https://doi.org/10.1016/j.biortech.2022.127039

Reis CER, Libardi Junior N, Bento HBS, Carvalho AKF, de Vandenberghe SLP, Soccol CR, Aminabhavi TM, Chandel AK (2023) Process strategies to reduce cellulase enzyme loading for renewable sugar production in biorefineries. Chem Eng J 451:138690. https://doi.org/10.1016/J.CEJ.2022.138690

Scott BR, Huang HZ, Frickman J, Halvorsen R, Johansen KS (2016) Catalase improves saccharification of lignocellulose by reducing lytic polysaccharide monooxygenase-associated enzyme inactivation. Biotechnol Lett 38:425–434. https://doi.org/10.1007/s10529-015-1989-8

Sharma G, Kaur B, Raheja Y, Agrawal D, Basotra N, Di Falco M, Tsang A, Chadha BS (2022) Lignocellulolytic enzymes from *Aspergillus allahabadii* for efficient bioconversion of rice straw into fermentable sugars and biogas. Bioresour Technol 360:127507

Simmons TJ, Frandsen KEH, Ciano L, Tryfona T, Lenfant N, Poulsen JC, Wilson LFL, Tandrup T, Tovborg M, Schnorr K, Johansen KS, Henrissat B, Walton PH, Lo Leggio L (2017) Dupree P (2017) Structural and electronic determinants of lytic polysaccharide monooxygenase reactivity on polysaccharide substrates. Nat Commun 81(8):1–12. https://doi.org/10.1038/s41467-017-01247-3

Tõlgo M, Hüttner S, Rugbjerg P, Thuy NT, Thanh VN, Larsbrink J, Olsson L (2021) Genomic and transcriptomic analysis of the thermophilic lignocellulose-degrading fungus *Thielavia terrestris* LPH172. Biotechnol Biofuels 14:131. https://doi.org/10.1186/s13068-021-01975-1

Vaaje-Kolstad G, Westereng B, Horn SJ, Liu Z, Zhai H, Sørlie M, Eijsink VGH (2010) An oxidative enzyme boosting the enzymatic conversion of recalcitrant polysaccharides. Science 330:219–222. https://doi.org/10.1126/science.1192231

Waterhouse A, Bertoni M, Bienert S, Studer G, Tauriello G, Gumienny R, Heer FT, de Beer TAP, Rempfer C, Bordoli L, Lepore R (2018) SWISS-MODEL: homology modelling of protein structures and complexes. Nucleic Acid Res 46:W296–W303. https://doi.org/10.1093/nar/gky427

Yan S, Xu Y, Yu XW (2021) From induction to secretion: a complicated route for cellulase production in *Trichoderma reesei*. Bioresour Bioprocess 8:107. https://doi.org/10.1186/s40643-021-00461-8

Zhang H, Han L, Dong H (2021a) An insight to pretreatment, enzyme adsorption and enzymatic hydrolysis of lignocellulosic biomass: experimental and modeling studies. Renew Sustain Energy Rev 140:110758. https://doi.org/10.1016/j.rser.2021.110758

Zhang X, Chen K, Long L, Ding S (2021b) Two C1-oxidizing AA9 lytic polysaccharide monooxygenases from *Sordaria brevicollis* differ in thermostability, activity, and synergy with cellulase. Appl Microbiol Biotechnol 105:8739–8759. https://doi.org/10.1007/s00253-021-11677-1